Susceptibility of Morpholine Substituents to Photo-oxidative Decomposition - Identification of Photo-Oxidative Degradants of Linezolid (PNU-100766)

Gary E. Martin*, Russell H. Robins, Phil B. Bowman, Wayne K. Duholke, Kathleen A. Farley#, Brian D. Kaluzny, Jane E. Guido, Sandra M. Sims, Thomas J. Thamann, and Brian E. Thompson

Pharmacia & Upjohn Pharmaceutical Development, Rapid Structure Characterization Group, Kalamazoo, Michigan 49001

Toshihide Nishimura, Yukimi Noro, and Tsutoma Tahara

Analytical Research & Specifications Development, Pharmacia & Upjohn Tsukuba-City, Ibaraki 300-42, Japan

June 1, 1998

Parenteral formulations of linezolid (PNU-100766), a novel (*S*)-3-(4'-fluorophenyl)-5-*N*-acetamidomethyloxazolidin-2-one antibiotic, were subjected to photo-stability testing as required by ICH guidelines. Direct, reversed phase chromatographic evaluation of the photo-irradiated solutions revealed two chromatographically broad degradants. Following preparative chromatographic isolation, the structures of both degradants were determined by mass spectrometric, nmr, and vibrational spectroscopic methods. The degradant structures formed by decomposition involving photo-oxidation of the morpholine, followed by a carbon-carbon bond scission to a formyloxyethylformamide-containing degradant. Facile hydrolytic cleavage of the formate ester in acidic media gave the second chromatographically broad degradant containing a *N*-2-hydroxyethylformamide group. The formamide substituent underwent further hydrolysis in acidic media to the corresponding secondary amine.

J. Heterocyclic Chem., **36**, 265 (1999).

Introduction.

Potent, orally active 5-acetamido-3-aryloxazolidin-2-one (DuP-721 and DuP105) antibiotics were first reported by researchers from DuPont in 1987 [1]. An oxazolidinone antibiotic discovery program initiated at The Upjohn Company subsequently led to the synthesis of two new oxazolidinone analogs, linezolid (PNU-100766, **1a**) and eperezolid (PNU-100592, **1b**) for the treatment of multiple antibiotic resistant Gram-positive bacterial infections in humans [2,3].

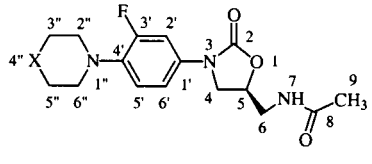

1a X = -O-
1b X = -NC(=O)CH_2OH

During stability evaluation of PNU-100766 (**1a**) parenteral solutions, photodecomposition studies were conducted as required by the ICH stability guidelines. In the course of these studies, two primary degradants were detected as broad peaks by analytical hplc methods. The isolation and spectroscopic characterization of these compounds suggested decomposition occurred *via* an initial oxidation of the morpholine substituent followed by the scission of the 2"-3" carbon-carbon bond to give the first degradant, which then hydrolytically decomposed to give the second. To the best of our knowledge, carbon-carbon bond cleavage within the morpholine substituent as described in this work has not been previously reported in the literature.

Results and Discussion.

Preliminary Structural Characterization.

Preliminary lc/ms characterization indicated molecular weights of 321 and 349 Da for the early- and late-eluting chromatographically broad peaks, respectively. Crude "isolates" of the two degradants obtained from the lc/ms waste stream were used to check for compound stability in dimethylsulfoxide, intended as an nmr solvent for larger samples isolated by preparative chromatography. Both compounds demonstrated adequate stability in dimethyl sulfoxide to allow the collection of one- and two-dimensional nmr spectral data. The early-eluting degradant, **4**, was somewhat more stable than the late-eluting component, **3**.

Identification of the Early-Eluting Degradant (**4**).

Interpretation of the eims and nmr data acquired for the early-eluting degradant indicated degradation had occurred solely in the morpholine moiety. Fragment ions in the eims for the loss of carbon dioxide from the oxazolidinone moiety (m/z 277), the loss of carbon dioxide plus the acetyl substituent (m/z = 234), and the loss of carbon dioxide plus the complete *N*-acetyl substituent (m/z 220) were observed. These fragments, shown in Figure 1 below, are indicative of

an intact oxzaolidin-2-one with an *N*-acetylmethylamino substituent. Likewise, the proton reference spectrum and a homonuclear TOCSY spectrum also confirmed that the oxazolidin-2-one and alkyl side chain were intact in the early-eluting degradant **4**. The homonuclear connectivity network was traced from the anisochronous 4-methylene protons (3.73/4.12 ppm) that correlate with the 5-methine resonance (4.71 ppm), which correlates, in turn, to the isochronous 6-methylene resonance (3.40 ppm), and finally to the 7-NH resonance (8.23 ppm). There were no neutral losses in the eims spectrum to unambiguously account for the defluorinated phenyl moiety. The proton reference spectrum, however, contained resonances for a four proton AB spin system (7.38/7.56 ppm) devoid of heteronuclear H-F couplings *in lieu* of the complex three proton multiplet characteristic of the parent drug. Mechanistically, it is unclear whether the fluorine was lost prior to or following 2",3" oxidation. Alternatively, the loss of the fluoro substituent may have also been concurrent to oxidation. Unless **2** (Scheme 1) can be isolated and its structure confirmed, there is no way to answer this question.

Two fragment ions observed in the eims spectrum account for the disruption of the morpholine ring. One fragment arises from a characteristic loss of CHO (m/z 293); a second arises from the loss of carbon dioxide and CHO (m/z 249) (see Figure 1 below). Both ions are unique relative to the parent drug. The nmr data also provided considerable insight into the nature of the photo-oxidative degradation of the morpholine ring. A proton singlet (8.36 ppm) directly bound to a carbon resonating at 162.1 ppm was observed in the GHSQC (gradient-HSQC) spectrum [4]. The one-dimensional ^{13}C-satellite spectrum showed this carbon to have a one-bond coupling constant ($^1J_{CH}$) of 197 Hz. Proton and carbon chemical shifts of this resonant pair are comparable to *N,N*-dimethylformamide which has a one-bond heteronuclear coupling constant of $^1J_{CH}$ = 192 Hz [5]. Resonances consistent with a β-hydroxyethylamino functionality were also observed. Concerted interpretation of the hrms, eims, and nmr data led to the structure shown by **4** (Figure 1 and Scheme 1).

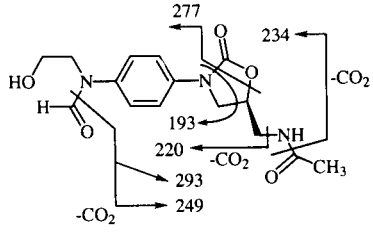

Figure 1. Mass spectral fragmentation pathways of the early eluting degradant, 4 formed by photo-oxidation of linezolid (PNU-100766).

Substantiation of the structure of **4** was provided by the GHMBC (gradient-HMBC) spectrum [6]. Long-range heteronuclear couplings reaffirmed the presence of an intact oxazolidin-2-one ring and located the *N*-acetylmethylamino group at the 5-position of the heterocycle. Correlations were observed which linked the H2" formamido proton to C6". Conversely, the H6" methylene protons were long-range coupled to the C2" formamido carbon and the C4' quaternary carbon in the phenyl ring. The latter served to indirectly establish the attachment of the morpholinyl nitrogen to C4'. Long-range couplings observed in the GHMBC spectrum of the early-eluting degradant are summarized in Figure 2 and serve to unequivocally establish the structure. For clarity, long-range responses within the aromatic ring have been omitted from **4** since none were crucial to the structure elucidation.

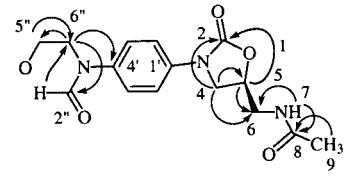

Figure 2. Long-range heteronuclear couplings observed in the GHMBC spectrum of **4**. Non-crucial long-range correlations within the 1,4-disubstituted phenyl are not included for clarity.

Finally, an infrared spectrum of the early-eluting degradant was also fully consistent with the structure shown by **4**. Absorbances were observed corresponding to the *N*-acetamide (C=O, 1663 and amide II, 1516 cm^{-1}), the carbamate linkage of the oxazolidin-2-one (C=O, 1746 and C-O, 1226 cm^{-1}), and the formamido carbonyl (1648 cm^{-1}). As expected, the absorbance for the C-F observed at 1116 cm^{-1} in the infrared spectrum of the parent was absent in **4**.

Identification of the Late-Eluting Degradant Structure (3).

The late-eluting degradant of **1a** was initially more challenging in that it exhibited instability to acid used as a modifier in the isolation of **4**. Isolation using acid-free conditions from irradiated feedstock, and from solutions of **1a** in vials charged with pure oxygen led to the isolation of samples that were stable and of sufficient quantity for characterization.

The eims of the late-eluting degradant, **3**, was nearly identical to that of **4**, exhibiting an additional 28 Da neutral loss, suggesting a structure containing an additional carbonyl. The proton nmr reference spectrum of the late-eluting degradant showed two singlets (8.16 and 8.38 ppm) in addition to the NH triplet (8.22 ppm). Resonances in the proton reference spectrum and correlations in the homonuclear TOCSY spectrum for the oxazolidin-2-one, the *N*-acetylmethylamino side chain, and resonances for the defluorinated 1,4-disubstituted phenyl substituent were observed at virtually identical chemical shifts to those of **4**.

These observations again suggested the morpholine ring as the site of photo-oxidative degradation.

The GHSQC spectrum showed that both of the proton singlets downfield were directly bound to ^{13}C (8.16/161.9 and 8.38/162.5 ppm), suggesting that both arose from an aldehyde, formamido, or formyl substituent. Morpholine fragments in the eims could be accounted for by successive losses of 28 Da (m/z 321 and 293) and by the concomitant oxazolidin-2-one decarboxylation (m/z 277 and 249), consistent with the presence of an additional H-C=O moiety in the structure.

Correlations observed in a GHMBC spectrum irrefutably established the structure of the late-eluting degradant as **3**. Incompletely canceled direct correlations exhibiting the one-bond heteronuclear coupling were strongly observed in the GHMBC spectrum for both of the downfield singlets. The 8.16/161.9 and 8.38/162.5 ppm (GHSQC) resonant pairs had one-bond heteronuclear couplings of 229 and 201 Hz, respectively (GHMBC). Observation of strong residual ^{13}C-coupled responses for the downfield singlets was not surprising given that the low-pass J-filter [7] used in the GHMBC [6] experiment was optimized for 160 Hz.

Based on analogy to the early-eluting degradant, the latter resonant pair was tentatively assigned to the H2"/C2" formamido group and confirmed by long-range couplings shown in Figure 3. The former resonant pair, with the larger one-bond heteronuclear coupling, was positioned in the structure on the basis of the long-range couplings in the GHMBC spectrum. The 8.16 ppm proton was long-range coupled only to a carbon resonating at 60.1 ppm (C5"). The protons attached to the 60.1 ppm carbon (GHSQC) resonated at 4.17 ppm and were coupled to the proton resonance at 4.02 ppm (H6", TOCSY). Conversely, the 4.17 ppm proton resonance was long-range coupled to the carbon resonance at 161.9 ppm (C3") and to the methylene carbon resonating at 43.1 ppm (C6"), which bore the protons resonating at 4.02 ppm. The 4.02 ppm proton resonance was long-range coupled to the C2" formamido carbon resonating at 162.5 ppm and to the aryl quaternary carbon resonating at 135.9 ppm (C4'). The formamido proton resonating at 8.38 ppm was long-range coupled to the methylene carbon resonance at 43.1 ppm (C6"). These connectivity pathways led to the assembly of the formyloxyethylformamide structure shown in Figure 3; the observed long-range couplings are summarized on the structure. Again, responses in the phenyl were omitted for clarity in since none were critical to the elucidation of the structure. It is noteworthy that the one-bond coupling extracted from the GHMBC spectrum for H3"/C3" of 229 Hz, is consistent with the measured one-bond coupling of ethyl formate, which was 226 Hz [5].

Mass spectral fragmentation, when interpreted in the context of the structure **3** established from the long-range heteronuclear connectivities obtained from the GHMBC spectrum, were easily rationalized as shown in Figure 4.

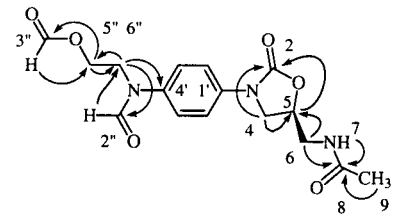

Figure 3. Long-range heteronulcear correlations observed in the GHMBC spectrum of **3**. Non-crucial correlations within the 1,4-disubstituted phenyl are omitted for clarity.

The infrared spectrum of the late-eluting degradant was consistent with structure **3**. Absorbances were observed corresponding to the *N*-acetamide (C=O, 1664 and amide II, 1517 cm^{-1}), the carbamate linkage of the oxazolidin-2-one (C=O, 1750 and C-O, 1225 cm^{-1}), the formamido carbonyl (1654 cm^{-1}), and a new absorbance for the formate ester carbonyl (1720 cm^{-1}). The absorbance for the C-F observed at 1116 cm^{-1} in the infrared spectrum of the parent molecule was again absent in **3**.

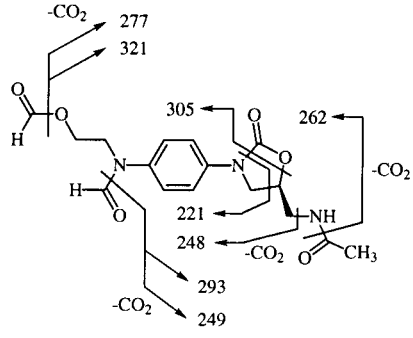

Figure 4. Mass spectral fragmentation pathways observed for the late-eluting degradant, **3**, formed during the photo-oxidation of linezolid (PNU-100766).

Formation of Photodegradants **3** and **4** from Parent Drug.

Immediately following the photoirradiation of solutions of linezolid (PNU-100766, **1a**), the resultant solution had a transient faint pink color suggestive of conjugated intermediates. Photo-oxidation leading to the formation of **3** and **4** invokes the "quinone-like" transient intermediate shown by **2** in Scheme I, although no direct evidence for **2** is available. Reductive scission of the carbon-carbon bond between the two carbonyl groups would lead to the formation of **3**. Following its formation, **3** can then be envisioned to degrade hydrolytically to **4**. To test this hypothesis, an nmr sample of **3** in dimethyl-d_6 sulfoxide was treated with one drop of 35% deuterium chloride in deuterium oxide warmed to 50°, and followed by analytical hplc. Within two hours, **3** had completely decomposed to form **4** and a new sharp chromatographic peak not observed during the initial photodegradation of the parent drug. First, these observations are

consistent with the instability of **3** observed when trifluoroacetic acid was used as a mobile-phase modifier during preparative-scale isolation of **4**. Second, our ability to isolate **3** when acid-free chromatographic mobile phases were employed is reasonable based on the observed acid instability of **3**. After six hours of exposure to deuterium chloride analytical hplc showed that **4** was also unstable, the intensity of the new chromatographic specie increased as the peak for **4** diminished. Preliminary eims data taken at six hours suggested that the product of the decomposition was the secondary amine, **5**, shown in Scheme I. Finally, after 72 hours, all traces of **4** were gone; the mass spectrum showed parent and fragment ions consistent with **5**, which was further confirmed by nmr following isolation.

Chromatographic Behavior.

The chromatographic behavior of **3** and **4** can be readily explained by considering their respective *gem*-diol hydrates, **6** and **7**. Equilibrium constants for the pairwise interconversion of **3** ⇔ **6** and of **4** ⇔ **7** comparable to the time scale of the hplc experiment would lead to a broadening of the chromatographic peaks. These structures also explain the improvement in chromatographic peak shape observed when the hplc column was heated to 40°. Close inspection of the esi/ms spectrum of **3** revealed a significant +18 Da adduct ion at m/z 368 indicative of *gem*-diol formation to yield **6**. The neutral loss (18 Da) spectrum of the m/z 368 ion clearly established the interrelation between the molecular weight of **3** and **6**, corresponding to the addition of water in the latter. Comparable hydration behavior can be invoked for the relationship between **4** and **7**. The observed poor chromatographic behavior of **3** and **4** was thus easily rationalized in terms of hydration behavior occurring on the chromatographic time scale.

Conclusions.

There have been no reports in the literature known to us describing the photo-oxidative decomposition of morpholine substituents *via* the pathway proposed in the present work. The proposed pathway accounts for the formation of the low level (<1%) photodecomposition products isolated and characterized. It would be difficult, however, to irrefutably confirm the proposed pathway unless **2** could be trapped and characterized. Hence, formation of **2**, or whatever specie serves as an intermediate in the formation of **3**, can only be inferred at this point on the basis of the faint pink coloration of solutions immediately following photoirradiation. It is prudent, regardless of the mechanistic chemistry involved, to consider protecting solutions of morpholine-containing pharmaceuticals from prolonged exposure to light. Furthermore, it should be noted that the compounds formed during the photo-oxidative degradation cascade in this study are not part of the existing impurity profile of linezolid. This study was conducted, as noted in the introduction, under ICH guidelines to assess the stability of the drug under severe photo-oxidative stress conditions. Under normal storage conditions, none of the compounds in the present study will be formed, nor will patients ever be exposed to any of the degradants characterized in this study.

Scheme I

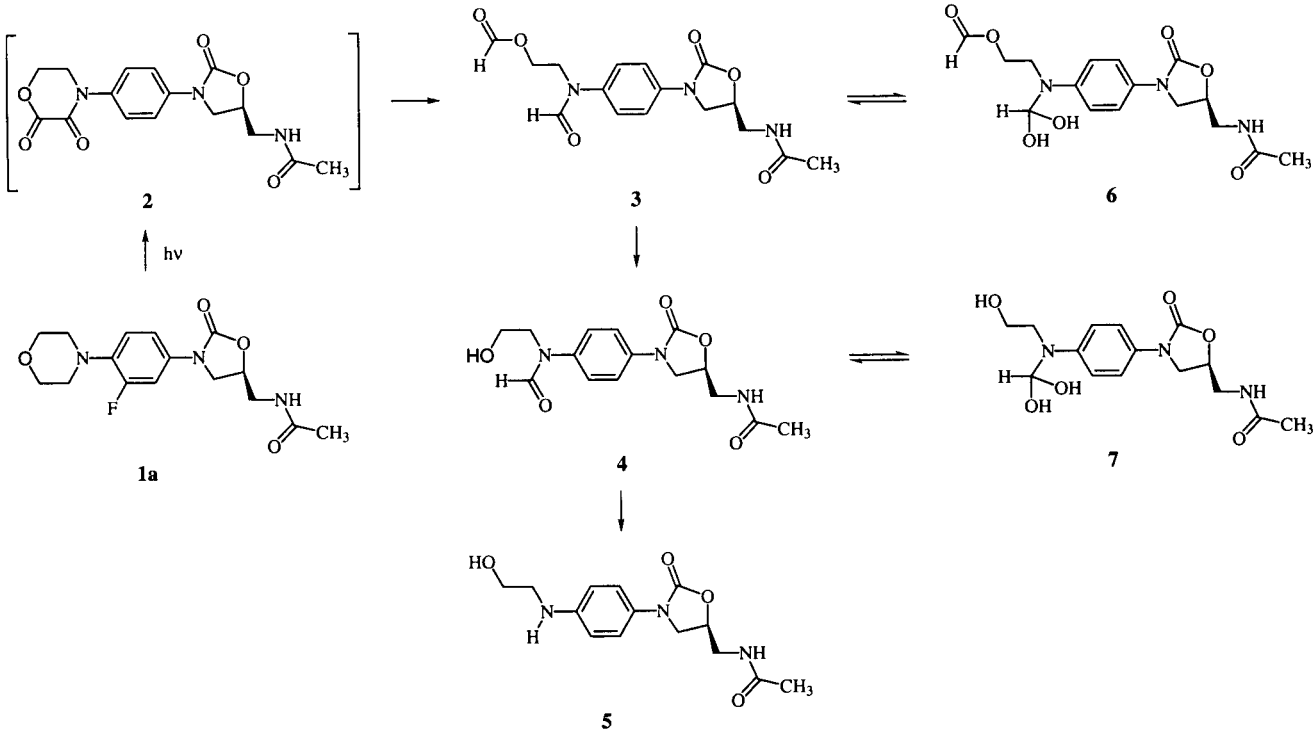

Table 1

Proton and Carbon Chemical Shift Comparison for Morpholine Photodegradants of PNU-100766 (**1a**) in Deuterodimethyl Sulfoxide

Position	δ^1H (ppm)			δ ^{13}C (ppm)		
	4	3	5	4	3	5 [c]
1	---	---	---	---	---	---
2	---	---	---	154.1	154.2	---
3	---	---	---	---	---	---
4	3.73	3.75	3.99	47.2 [b]	47.3	47.8
1	4.12	4.12	3.62			
5	4.71	4.72	4.61	71.5	71.6	70.8
6	3.40	3.41	3.37	41.4	41.5	41.0
7NH	8.23	8.22	8.20	---	---	---
8	---	---	---	169.9	170.0	---
9-CH_3	1.82	1.82	1.82	22.4	22.5	22.1
1'	—	---	—	136.8 [a]	136.9	---
2'/6'	7.56	7.58	7.19	118.8	118.9	111.6
3'/5'	7.38	7.39	6.58	124.3	124.5	120.4
4'	---	—	—	136.5 [a]	135.9	---
1"NH	---	---	5.42	---	---	---
2"	3.76	4.02	3.05	47.1 [b]	43.1	45.3
3"	3.46	4.17	3.52	57.7	60.1	59.3
4"OH	3.68	---	3.65	---	---	---
5"	---	8.16	---	---	161.9	---
					^{1}JCH = 229 Hz [e]	
6"	8.36	8.38	---	162.1	162.5	---
				^{1}JCH = 197 Hz [d]	^{1}JCH = 201 Hz [e]	

[a], [b] Resonance assignments may be transposed, pairwise. [c] Carbon chemical shifts obtained from GHSQC spectrum, no data were available for quaternary carbons since a direct observe ^{13}C spectrum was not acquired. [d] One-bond coupling constant measured from a one-dimensional ^{13}C satellite spectrum. [e] One-bond coupling constants measured from residual direct responses in the GHMBC spectrum.

Finally, it is interesting to note that the structural moiety produced in the degradation of the morpholine substituent of **1a** to give **3** is not without structural precedent in the literature. For example, a compound analogous to **3**, (-)-*N,O*-diformylnorephedrine, was formed as a minor component of a reaction to prepare an authentic sample of *N*-formylnorephedrine. The *N*-formylnorephedrine was synthesized for comparison to a sample of this alkaloid isolated from a natural source [8]. Formyloxyethylformamides have also been periodically utilized as chemical synthons in the elaboration of various heterocycles [9,10] as potential pharmaceuticals.

EXPERIMENTAL

Feedstock.

Photolytic degradant **4** was isolated from 2 mg/ml parenteral sterile solution lots which had been photolyzed for 50 days in a Lightron (Nagano Science TP-1293) light cabinet at 1000 lux (fluorescent tubes). Photolytic degradant **3** was isolated from the same solutions which had been exhaustively purged with oxygen prior to photolysis for 18 hours in a SunTest light cabinet at 2000 lux. Oxygen treatment was employed to enhance the formation of **3** during photolysis.

Analytical Chromatography.

Analytical hplc analysis of photolyzed parenteral solutions and degradant isolates was performed using a Hewlett-Packard HP1090 chromatographic system with fixed wavelength uv absorbance detection at 254 nm. Separations were achieved with a 4.6 x 150 mm MACMOD Zorbax RX™ C8 (5 micron) column using a 0.1% trifluoroacetic acid modified acetonitrile/water linear gradient from 10 to 75% acetonitrile over 35 minutes at a flow rate of 1.0 ml/minute. All samples were analyzed without pretreatment. The photolysis products of interest eluted as broad bands near 13 (**4**) and 21 (**3**) minutes and the chromatographically well behaved parent compound near 27 minutes. On-line analytical hplc/ms was similarly performed using an LDC Analytical Constametric 4100 series chromatograph with serial mass spectral detection described below. The hplc analysis was performed at ambient and elevated (40°) temperature to examine the thermal dependence of the broad bands of interest.

Preparative Chromatography.

Preparative hplc isolation of **4** was performed by injecting 50 ml aliquots of neat feedstock onto a 60 x 250 mm Kromasil™ C18 (10 micron) column followed by elution with a 0.1% trifluoroacetic acid modified acetonitrile/water linear gradient from 10-20% acetonitrile over 25 minutes at a flow rate of 102 ml/minute. Pooled fractions were lyophilized to remove solvent yielding an oily tan-colored crude isolate of **4**. To improve purity, the crude isolated was redissolved in mobile phase and subjected to a second chromatographic pass using a 20 x 250 mm Kromasil C8 (10 micron) column of greater efficiency at a flow rate of 17 ml/min. Resultant second pass fractions were diluted with Milli-Q™ (Millipore Corp.) water, concentrated, desalted, and reduced in chemical interferences *via* trapping on a Hamilton PRP-1 column. The eluant from the trapping column was lyophilized to yield about 0.5 mg of **4** having a peak area percent purity of 93.5% by the analytical hplc.

Photolysis product **3** was similarly isolated from oxygenated feedstock using a non-acidic semi-preparative hplc method using and acetonitrile/water linear gradient and a 20 x 250 mm Kromasil C18 (10 micron) column at a flow rate of 20 ml/min. The exclusion of acid was necessary to preclude rapid secondary degradation of **3** during preparative work-up. Pooled fractions were rotary evaporated, diluted with milli-Q water, concentrated, desalted, and reduced in chemical interferences using the Hamilton PRP-1 trapping column as described above. The trap eluant was lyophilized to yield several milligrams of **3** with a peak area percent purity of 98.6% by analytical hplc.

Mass Spectrometry.

On-line APCI (Atmospheric Pressure Chemical Ionization) and ESI (Electrospray Ionization) mass spectra of **3** and **4** were recorded at nominal mass resolution using a Finnigan TSQ-700 series triple quadrupole mass spectrometer and associated interface of inhouse construction [11]. "Ultra-soft" ESI primary ionization neutral loss (18 AMU) ms/ms experiments were performed to substantiate the equilibrium hydration of the formamido functionality of **3** under chromatographic conditions as an explanation of the poor (broad) chromatographic behavior observed. EI (Electron Ionization) mass spectra of isolates were recorded at 70 eV using a Finnigan 4600 series single stage quadrupole mass spectrometer operating at nominal mass resolution. Solid isolates were volatilized by ballistic heating from ambient to 400° at 10°/second using the associated Direct Expose Probe (DEP). Empirical formulae for **3** and **4** were determined by accurate mass measurement using a Kratos MS-50RF Nier-Johnson double focusing spectrometer operating at a resolution of 20,000 (10% valley definition) in the peak-matching mode. Samples were prepared by dissolving a small portion of each isolate in glycerol (Aldrich) matrix prior to LSIMS (Liquid Secondary Ion Mass Spectrometry). The protonated molecular ion for each isolate was peak matched to the $(gly)_3H^+$ matrix cluster ion at m/z=277.149857.

NMR Spectrometry.

All nmr spectra were recorded using samples prepared by dissolving approx. 0.5 mg of isolated material in 0.15 or 0.5 ml 99.96% dimethyl-d_6 sulfoxide (Isotec) under an inert argon atmosphere. Proton, homonuclear TOCSY, and heteronuclear shift correlation experiments (GHSQC [4] and GHMBC [6]) were performed using a Bruker AMX-400 spectrometer equipped with either a Nalorac 3 mm gradient micro inverse (**4**) or Bruker **5** mm single axis gradient inverse triple resonance probe (**3** and **5**). Carbon spectra were recorded using a Bruker AMX- 500 spectrometer equipped with either a Nalorac 3 mm micro dual (**4**) or 5 mm Bruker dual probe (**3** and **5**).

Homonuclear TOCSY spectra were acquired as 1024 x 128 or 1024 x 256 point files using a mixing times of 17.4 or 18.5 msec; data were zero-filled to either 1024 x 1024 or 2048 x 512 points during processing. The GHSQC data were acquired as a 2048 x 128 or 2048 x 160 point files with the delay for the one-bond coupling optimized at 145, 150, or 160 Hz. Delays were optimized on the basis of an assumed average one-bond heteronuclear coupling of 160 Hz to allow responses for both aliphatic (J ~ 125-140 Hz) and formyl (J ~ 197-229 Hz) species to be observed. Long-range heteronuclear correlations were determined using the GHMBC experiment [6] in which the long-range delay was optimized for 70 or 64 msec. GHMBC data were acquired as either 1024 x 256 or 2048 x 320 point files and were processed using a shifted sine and cosine multiplication before the first and second Fourier transforms, respectively.

Infrared Spectroscopy.

Samples **3** and **4** were prepared by placing two drops of the residual dimethyl-d_6 sulfoxide nmr sample on potassium bromide plates followed by solvent removal with a stream of nitrogen. The plates were interrogated on a Spectratech microscope stage interfaced to a Nicolet 60-SX spectrometer equipped with a MCT-B detector. Data were collected from 4000 to 400 cm^{-1} at 2 cm^{-1} resolution; the spectra were obtained by summing 500 scans. All data were processed as a Fourier transform utilizing a Happ-Genzel apodization function and plotted as absorbance vs. frequency.

REFERENCES AND NOTES

Present address: SAMChem, Pharmacia & Upjohn Kalamazoo, MI.

[1] A. M. Slee, M. A. Wuonola, R. J. McRipley, I. Zajac, M. J. Zawanda, P. T. Bartholomew, W. A. Gregory, and M. Forbes, 27th Interscience Conference on Antimicrobial Agents and Chemotherapy, 244 (1987); A. M. Slee,, M. A. Wuonola, R. J. McRipley, I. Zajac, M. J. Zawanda, P. T. Bartholomew, W. A. Gregory, and M. Forbes, *Antimicrob. Agents Chemother.*, **31**, 1791 (1987).

[2] S. J. Brickner, D. K. Hutchinson, M. R. Barbachyn, P. R. Manninen, D. A. Ulanowicz, S. A. Garmon, K. C. Grega, S. K. Hendges, D. S. Toops, C. W. Ford, and G. E. Zurenko, *J. Med. Chem.*, **39**, 673 (1995).

[3] G. E. Zurenko, B. H. Yagi, R. D. Schaadt, J. W. Allison, J. O. Kilburn, S. E. Glickman, D. K. Hutchinson, M. R. Barbachyn, and S. J. Brickner, *Antimicrob. Agents. Chemother.*, **40**, 839 (1996).

[4] G. W. Vuister, R. Boelens, R. Kaptein, R. E. Hurd, B. K. John, and P. C. M. van Zilj, *J. Am. Chem. Soc.*, **113**, 9688 (1991); J. Ruiz-Cabello, G.W. Vuister, C. T. W. Moonen, P. van Geldern, J. S. Cohen, and P. C. M. van Zilj, *J. Magn. Reson.*, **100**, 282 (1992).

[5] E. R. Malinowski, L. Z. Pollara, and J. P. Larmann, *J. Am. Chem. Soc.*, **84**, 2649 (1962).

[6] A. Bax and M. F. Summers, *J. Am. Chem. Soc.*, 108, 2093 (1986); R. E. Hurd and B. K. John, *J. Magn. Reson.*, **91**, 648 (1991).

[7] H. Kogler, O. W. Sørensen, G. Bodenhausen, and R. R. Ernst, *J. Magn. Reson.*, **55**, 157 (1983).

[8] I. A. AI-Meshal, M. Nasir, and F. S. EI-Feraly, *Phytochemistry*, **25**, 2241 (1986).

[9] A. V. Germash, V. V. Zorin, A. A. Lapshova, S. S. Zlotskii, and D. L. Rakhmankulov, *Zh. Prikl. Khim.*, **57**, 1187 (1984); *Chem. Abstr.*, **102**, 5673 (1985).

[10] Y. Furukawa, O. Miyashita, and S. Shima, *Chem. Pharm. Bull.*, **24**, 970 (1976).

[11] R. H. Robins, U.S. Patent No. 5,235,186; assigned to Finnigan, Inc., San Jose, CA.